

See discussions, stats, and author profiles for this publication at: <https://www.researchgate.net/publication/303683780>

Inorganic Transport through Composite Geosynthetics and Compacted Clay Liners under Geomembranes with Multiple Defects

Article in *Australian Geomechanics Journal* · March 2016

READS

12

3 authors:



[Abbas El-Zein](#)

University of Sydney

87 PUBLICATIONS 584 CITATIONS

[SEE PROFILE](#)



[Ingrid Mccarroll](#)

University of Sydney

4 PUBLICATIONS 10 CITATIONS

[SEE PROFILE](#)



[Mohsen S Masoudian](#)

University of Nottingham

15 PUBLICATIONS 34 CITATIONS

[SEE PROFILE](#)

INORGANIC TRANSPORT THROUGH COMPOSITE GEOSYNTHETICS AND COMPACTED CLAY LINERS UNDER GEOMEMBRANES WITH MULTIPLE DEFECTS

Abbas El-Zein¹, Ingrid McCarroll², Mohsen Masoudian³

1 Associate Professor, School of Civil Engineering, University of Sydney, NSW 2006, Australia. Email: abbas.elzein@sydney.edu.au; corresponding author

2 PhD Candidate, School of Aerospace, Mechanical and Mechatronics Engineering, University of Sydney, NSW 2006, Australia.

3 Post-Doctorate Researcher, School of Civil Engineering, University of Sydney, NSW 2006, Australia.

ABSTRACT

Geosynthetic clay liners (GCLs) and compacted clay liners (CCLs) are widely used in waste containment systems – usually in conjunction with a high-density polyethylene geomembrane – for the protection of groundwater from contamination. Defects in geomembranes have been shown to have detrimental impacts on their performances. These systems, including defects, have been studied mostly through the lens of hydraulic leakage. Previous contaminant migration studies of liner systems have assumed single rather than multiple defects or have simulated organic, rather than inorganic transport when multiple defects are present. Unlike organic chemicals, inorganic contaminants do not biologically decay and have extremely small coefficients of diffusion through the intact parts of the geomembrane. These differences create different transport regimes, with contaminant levels likely to take longer to build up and dissipate in the aquifer. This paper simulates the transport of inorganic contaminants in systems containing CCLs or GCLs, under a geomembrane with multiple defects. Specifically, we aim to a) assess the extent to which leakage rates are good predictors of concentrations of inorganic contaminants in the aquifer and b) quantify the relative effect of various design and field parameters on the degree to which defects in the geomembranes reduce the performance of these systems.

Two-dimensional models of liner systems with multiple defects are simulated with the finite-element based Soil Pollution Analysis System (SPAS) for the transport of chloride and cadmium in geosynthetic and compacted composite clay liners. The coupled, steady-state seepage equations and time-dependent reactive diffusion advection equations are solved in two-dimensional space in order to compute seepage velocities and chemical concentrations in the system, including the underlying aquifer. A finite mass boundary condition is applied at the top of the system, representing a finite intake of contaminants in the waste. Parametric analyses are conducted to characterise the relationship between, on the one hand, various design and field parameters (intake of contaminant, thickness of primary liner, frequency and size of defects, hydraulic conductivities of clay) and, on the other hand, leakage rates and maximum concentrations of contaminant in the aquifer.

We find that defects in the geomembrane lead to significant increases in maximum concentrations of inorganic contaminants in the aquifer. However, these maxima are predicted to occur a few hundred years after the closure of the landfill, i.e. beyond the usual regulatory limit of the design. Design/field parameters with the strongest effect on maximum contaminant levels in the aquifer are the hydraulic conductivities of the primary liner (CCL or GCL), the frequency of defects and, in the case of the CCL, the thickness of the primary liner. Finally, we find that leakage rates are sometimes poor indicators of the effects of design parameters on chemical concentrations in groundwater. The maximum specific discharge rate under defects can have an important effect on concentrations as well, though it is not usually taken directly into account, nor is it easily measurable.

Keywords: geosynthetic clay liners, compacted clay liners, contaminant transport, geomembranes, chloride, cadmium, inorganic, finite element method

1. INTRODUCTION

One of the challenges facing designers and operators of landfill liners is to ensure that the liner will perform its insulation function over decades and centuries, keeping concentrations of contaminants in groundwater below acceptable thresholds, well after the facility has ceased to receive waste. The difficulty lies in the fact that some contaminants, particularly inorganic ones, can persist for a long time in the waste and may migrate at extremely slow rates through the clay barrier, eventually breaking through into the groundwater. Monitoring chemical leaching and detecting any leakages are one way in which engineers approach this problem. However, the remediation of a faulty design can be very costly and landfill designers are hard pressed to ensure that such leakage is kept to a minimum.

Most landfill liners at present include, in addition to a compacted clay liner (CCL) or a geosynthetic clay liner (GCL), a high density geomembrane which is extremely effective in preventing water and inorganic contaminants from

travelling from the waste into the subsurface (Rowe et al., 2004). However, given the large surface areas over which the liner is deployed and the challenging chemical, physical and climate environment in which it must operate, it is very difficult to prevent damage from occurring to the geomembrane before, during and after waste placement, which leads to some leakage into the underlying layers (e.g., Nosko and Touze-Foltz, 2000). Traditionally, much attention has been given to the hydraulic conductivity of the clay and geosynthetic liners because of the risk of catastrophic increases in conductivity as a result of chemical and/or thermal interactions with the waste (e.g., Azad et al., 2012; Abuel-Naga et al., 2013). Correspondingly, hydraulic leakage has been used as a measure of performance and regulators typically mandate limits on the maximum leakage allowed. A number of authors developed closed-form equations and analytical techniques for evaluating leakage rates (Wilson-Fahmy and Koerner, 1995; Giroud and Touze-Foltz, 2005; Rowe, 2005). However, less attention has been given to chemical concentrations (Rowe, 2005; Abuel-Naga and Bouazza, 2009; El-Zein and Rowe, 2008; El-Zein and Touze-Foltz, 2010).

Foose et al. (2002) modelled seepage and contaminant transport through a composite liner and idealised boundary conditions, considering a single defect and focusing in their analyses on flux rates rather than pollutant concentrations. Rowe and Brachman (2004) simulated the transport of organic and inorganic compounds under 1D conditions assuming an average leakage rate, rather than multiple defects, with the aim of comparing the performances of CCL and GCL liners. El-Zein and Rowe (2008) and El-Zein and Touze-Foltz (2010) conducted 2D finite element analyses of the coupled hydrochemical equations for multiple defects and identified conditions under which leakage rates do not correlate well with levels of organic contamination in groundwater. El-Zein et al. (2012) extended the analysis into 3D in order to evaluate the effects of downstream boundary conditions and groundwater flow direction on organic contamination. Kandris and Pantazidou (2012) conducted parametric analyses for flow and transport through liners with defects, using one-dimensional empirical and analytical solutions. However, to date, no attempt has been made in 2D or 3D to simulate the chemical transport of inorganic material through liners with multiple defects and assess the effects of different design or field parameters under such scenarios. Unlike organic chemicals, inorganic ones do not biologically decay and, in practice, do not diffuse through the intact parts of the geomembrane. These differences create different transport regimes, with pollution levels in the aquifer taking longer to build up and dissipate.

This paper extends our work on organic pollutants to inorganic contaminants, specifically aiming to

- a) quantify the effects of various design parameters on leakage rates and concentrations of inorganic contaminants in the aquifer in order to identify those parameters with the biggest impact on the liner's performance, and
- b) assess the extent to which leakage rates are good predictors of inorganic solute concentrations in the aquifer.

Two-dimensional models of liner systems with multiple defects are simulated with the finite-element based Soil Pollution Analysis System (SPAS) for the transport of chloride and cadmium. The coupled, steady-state seepage equations and time-dependent reactive diffusion advection equations are solved in order to generate seepage velocities and chemical concentrations in the system, including the underlying aquifer. A finite mass boundary condition is applied at the top of the system, representing a finite intake of contaminants in the waste. Parametric analyses are conducted to characterise the relationship between, on the one hand, various design and field parameters (intake of contaminant, thickness of layers, flow and transport parameters, frequency and size of defects) and on the other hand maximum concentration of contaminant in the aquifer.

2. METHODS

2.1 GOVERNING EQUATIONS OF SEEPAGE AND CONTAMINANT TRANSPORT

The steady-state flow of water in saturated, incompressible soil can be represented by the following equations, based on Darcy's law and a mass conservation statement:

$$k_x \frac{\partial^2 H}{\partial x^2} + k_y \frac{\partial^2 H}{\partial y^2} = 0 \quad (1)$$

$$v_{ax} = -k_x \frac{\partial H}{\partial x} \quad (2)$$

$$v_{ay} = -k_y \frac{\partial H}{\partial y} \quad (3)$$

$$v_x = \frac{v_{ax}}{n} \quad (4)$$

$$v_y = \frac{v_{ay}}{n} \quad (5)$$

$$|\mathbf{v}| = \sqrt{v_x^2 + v_y^2} \quad (6)$$

where (x,y) is a Cartesian coordinate system [L], H is the total hydraulic head [L], k_x , k_y are the two diagonal components of the hydraulic conductivity tensor [$L.T^{-1}$], v_x and v_y are the two components of the seepage velocity vector [$L.T^{-1}$], $|\mathbf{v}|$ is the magnitude of the seepage velocity [$L.T^{-1}$], v_{ax} and v_{ay} are the two components of the Darcy velocity vector [$L.T^{-1}$], and n is the porosity. A set of boundary conditions for equation (1) can be expressed by:

$$m_1 H + m_2 v_\eta = m_3 \quad (7)$$

where v_η is the component of seepage velocity normal to the boundary, and m_1 , m_2 and m_3 are given coefficients.

Where the transport of inorganic, non-radioactive species dissolved in soil water is governed by mechanical dispersion, molecular diffusion, advection and linear sorption, it can be described by the following set of equations:

$$\frac{\partial}{\partial x} \left(n D_{xx} \frac{\partial c}{\partial x} \right) + \frac{\partial}{\partial x} \left(n D_{xy} \frac{\partial c}{\partial y} \right) + \frac{\partial}{\partial y} \left(n D_{yx} \frac{\partial c}{\partial x} \right) + \frac{\partial}{\partial y} \left(n D_{yy} \frac{\partial c}{\partial y} \right) \quad (8)$$

$$- n v_x c - n v_y c = (n + \rho K_d) \frac{\partial c}{\partial t}$$

$$D_{xx} = D_0 + \alpha_T |\mathbf{v}| + (\alpha_L - \alpha_T) \frac{v_x^2}{|\mathbf{v}|} \quad (9)$$

$$D_{xy} = D_{yx} = (\alpha_L - \alpha_T) \frac{v_x v_y}{|\mathbf{v}|} \quad (10)$$

$$D_{yy} = D_0 + \alpha_T |\mathbf{v}| + (\alpha_L - \alpha_T) \frac{v_y^2}{|\mathbf{v}|} \quad (11)$$

$$f_x = -n D_{xx} \frac{\partial c}{\partial x} + n v_x c \quad (12)$$

$$f_y = -n D_{yy} \frac{\partial c}{\partial y} + n v_y c \quad (13)$$

where t is time [T], $c(t,x,y)$ is the solute concentration [$M.L^{-3}$], D_{xx} and D_{yy} are the two diagonal components of the hydrodynamic dispersion tensor for the solute in the medium [$L^2.T^{-1}$], D_0 is the coefficient of molecular diffusion of the solute in the soil water [$L^2.T^{-1}$], α_L and α_T are the longitudinal and transverse dispersivities, respectively [L]; K_d is the linear sorption distribution coefficient of the solute in the medium [$L^3.M^{-1}$], ρ is the dry density of the soil [$M.L^{-3}$], f_x and f_y are the solute fluxes, or specific discharges, in the two directions [$M.L^{-2}.T^{-1}$]. A general form of a set of boundary conditions for equation (8) is given by:

$$m_4 c + m_5 f_\eta = m_6 \quad (14)$$

where f_η is the flux of contaminant normal to the boundary, and m_4 , m_5 and m_6 are given coefficients. Another boundary condition of interest is one in which a finite mass of contaminants is specified. In this study, we simulate this by including a layer of soil with specified initial concentration of the contaminant. The depth of the layer is chosen so as to reflect the amount of contaminant present in the layer.

A composite landfill liner is a multilayered system. Flow and chemical transport through it can be modelled by solving equations (1) and (8), specifying different material properties for the respective layers. However, the interface between the geomembrane and the primary liner requires special attention, on two accounts. First, surface sorption on the geomembrane can be an important partitioning process affecting the way contaminants travel through the geomembrane. However, this is of more consequence for organic than inorganic contaminants because geomembranes are practically impervious to the latter and the process will therefore be neglected here. Second, the quality of contact between the geomembrane and the underlying primary liner is known to affect leakage rates through defects in the former (Rowe et al., 2004). Poor contact allows more water to build up between the two layers, leading to stronger downward Darcy velocities. This effect can be modelled by introducing a layer between the geomembranes and the

primary liner that is at least one order of magnitude thinner than either (El-Zein and Rowe, 2008). The quality of contact is characterised by the hydraulic transmissivity θ_x in the horizontal direction, defined as:

$$\theta_x = k_x t_t \quad (15)$$

where t_t is the thickness of the transmissive layer. Higher transmissivities imply wider lateral penetration of leachate under the geomembrane and more leakage.

2.2 SIMULATION MODELS

The Soil Pollution Analysis System (SPAS) is a purpose-built finite element method (FEM) program in 2D and 3D which simplifies the generation of landfill liner features (El-Zein and Balaam, 2012). It is based on a weighted-residual Galerkin solution of the above equations using polynomial or exponential discretisations (El-Zein, 2005). Two approaches to time discretisation are used, a time-marching (TMFEM) scheme and Laplace transform (LTFEM) scheme (El-Zein and Booker, 1999; El-Zein et al., 2005). The former is more general in scope because, unlike the latter, it allows all input parameters to change in time. However, the LTFEM is more computationally efficient and can generate the entire time history of the problem in a few seconds of CPU time. The LTFEM is adopted here because input parameters are assumed to be constant in time. Two degrees of freedom are present at each node: the total hydraulic head H and the solute concentration C . H , v_x , v_y , v_{ax} , and v_{ay} are first obtained from the steady-state seepage analysis. Next, the seepage velocities become part of the input parameters for the time-dependent mass-transport problem which, when solved, yields C , f_x and f_y . Leakage rates are calculated as the integral of the vertical Darcy velocity function (v_{ay}) over the interface between the primary liner and the attenuation layer, divided by the surface area of that interface.

The hydraulic steady-state assumption is justified because of the long time scales (decades and centuries) of solute transport processes in clay soils. Both LTFEM and TMFEM implementations have been validated through extensive comparisons to analytical and numerical solutions from the literature (e.g., Ogata and Banks, 1961; Booker and Rowe, 1987; El-Zein, 2008). In order to characterise the relationship between landfill liner design parameters and contamination levels in groundwater, four base cases are established:

- chloride transport through a composite compacted clay liner (CCL-Cl);
- cadmium transport through a composite compacted clay liner (CCL-Cd);
- chloride transport through a composite geosynthetic clay liner (GCL-Cl);
- cadmium transport through a composite geosynthetic clay liner (GCL-Cd).

Chloride is adopted because data on its diffusion properties are widely available and it has negligible sorption capacity in soil, leading to fewer variables in the analyses and a worst-case scenario. Cadmium on the other hand is a heavy metal with some sorptive affinity to clay and known diffusion parameters. All base cases are made of a 1.5mm geomembrane (GM), a primary liner (PL), i.e. a CCL or a GCL, an attenuation layer and a 1m aquifer. A cross-section of the model is shown in Figure 1.

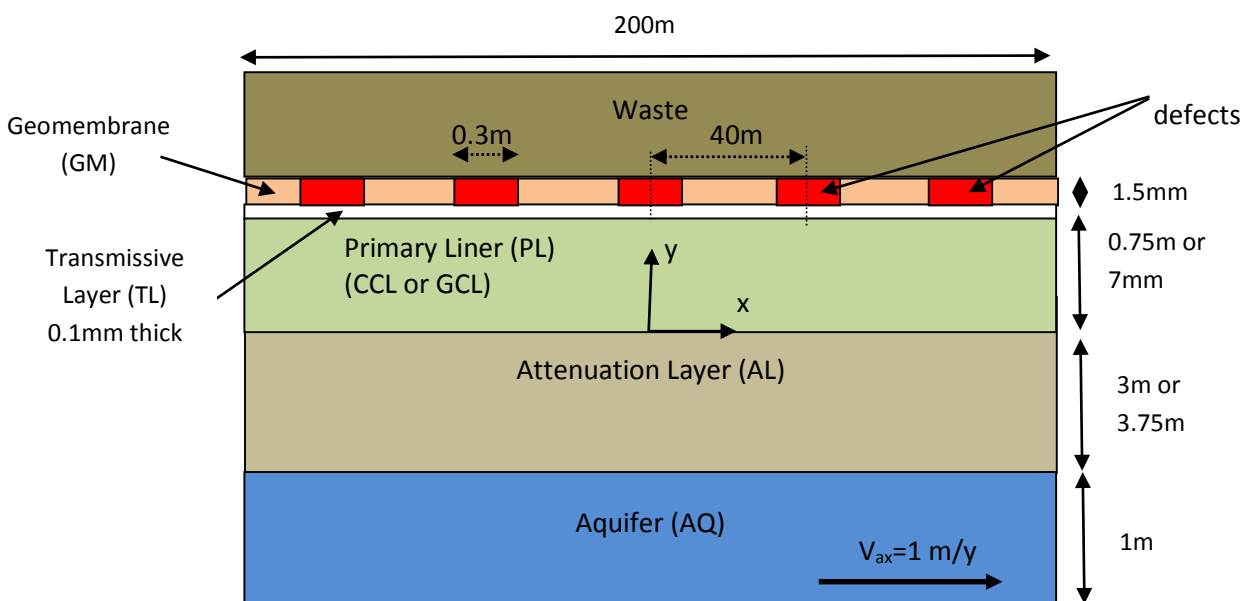


Figure 1. Cross-section of base model of landfill liner-soil system (not to scale; origin of the axes at the centre of the lower surface of the primary liner)

The CCLs in base cases a and b are 75cm deep, while the GCLs in base cases c and d are in a standard 7mm thickness. In order to maintain the same overall thickness of liners in all four cases, the AL is 3m deep in cases a and b and 3.75m deep in cases c and d. All liners are 200m wide in the x direction (simulated in 2D). The out-of-plane z dimension of the landfill is assumed to be 100m long for the purpose of calculating density of defects. Five equally-spaced rectangular defects are present on the geomembrane in all base cases, yielding a density of 2.5 defects per hectare. Given the 2D nature of the analyses, the defects are assumed to extend all along the z-direction (i.e., the axis normal to the cross-section shown in Figure 1). In the chemical transport analyses, the contaminants are assumed to be in direct contact with the primary liner of the area of the defects. Flow in the aquifer is assumed to be in the x direction at a Darcy velocity of 1 m/year. Material properties used in the base cases are shown in Table 1.

Transmissivities of 10^{-10} m²/s for the GCL and 1.6×10^{-8} m²/s for the CCL are adopted. The thickness of the high-density polyethylene (HDPE) geomembrane is assumed to be 1.5 mm with leaking wrinkles of 0.3m width (i.e., defect width), as observed by Pelte et al. (1994). This is consistent with works by Touze-Foltz et al. (2001) and Chappel et al. (2008). All layers are fully saturated and the aquifer is assumed to be 1m deep. Sorption in all layers is negligible, except for cadmium in the primary liner. Sorption in the attenuation layer can be an important mechanism through which contamination is retarded. However, the rates of sorption vary with different types of soils and it is assumed to be nil in this study, in order to remain on the conservative side. Pressure heads of 30cm are applied at each defect, and 3.75m in the aquifer. All other surfaces have zero flow hydraulic boundary conditions. For the chemical transport problem, initial contaminant concentrations are taken to be identically zero, everywhere except in the waste. To simulate a specified mass of contaminants at the inlet, a waste layer is included in the mass transport problem with a specified initial concentration C_0 and a thickness equal to the equivalent height of leachate H_f . H_f is a function of C_0 as well as the waste surface density d [M.L⁻²] and the contaminant density in the waste p_0 [M.M⁻¹] where

$$H_f = \frac{dp_0}{C_0} \quad (16)$$

C_0 , d , p_0 and H_f for the four base cases are shown in Table 1. At the downstream edge of the aquifer, an advective discharge boundary condition is applied, i.e. contaminants are assumed to leave the system at a flux rate of $nv_x c$. All other surfaces have zero flux boundary conditions. Leakage rates are calculated as:

$$L = \frac{1}{A} \int_A v_{ay} dA \quad (17)$$

where A is the surface at the interface between the PL and the AL. The analyses are conducted in 2 stages. First, the four base cases are analysed as benchmark references. Second, the effect on leakage rates and chemical concentrations in the aquifer of the following parameters is studied: thickness of primary liner t_{AL} ; hydraulic conductivities of primary liners and attenuation layers, k_{PL} and k_{AL} ; transmissivity θ_x ; diffusion coefficients in the liner and the attenuation layer, D_{PL} and D_{AL} ; equivalent height of leachate in the waste H_f ; and defect width w and frequency f . The effects of the geomembrane thickness have also been analysed; however, they have been found to be negligible because of the very low conductivity of geomembranes to water and inorganic contaminants.

SPAS generates the finite element mesh automatically, including refinements around defects, to avoid numerical oscillations as a result of large values of Darcy velocities (see typical mesh used in Figure 2). Convergence analyses have been conducted to ensure robustness of predictions. In all simulations, 8-noded quadratic elements are used.

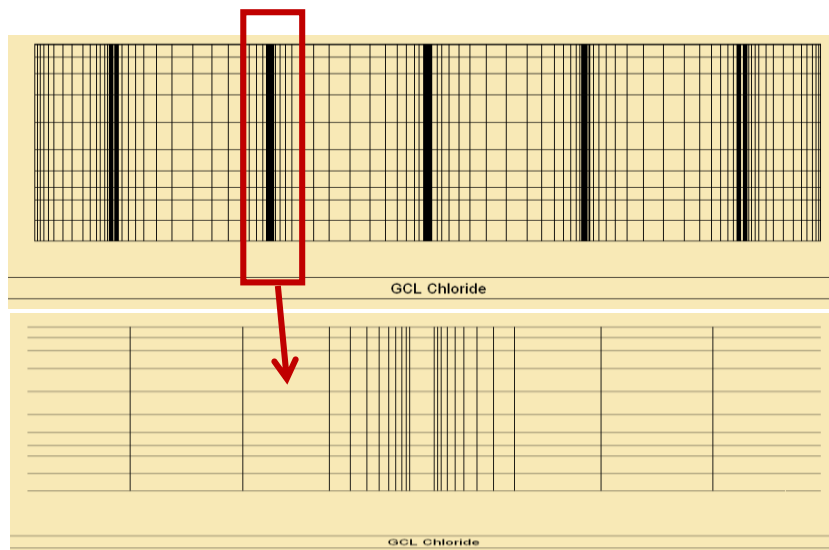


Figure 2. Typical finite element mesh used in the analyses

Table 1: Parameters Used in Simulations : Four Base Cases

Item	Description	Units	Source	a: CCL-Cl	b: CCL-Cd	c: GCL-Cl	d: GCL-Cd
C_0	Initial concentration in the waste	g/m ³	[1] p56	11950	0.05	11950	0.05
d	Waste density	g/m ²	[2]	2.5×10^7	2.5×10^7	2.5×10^7	2.5×10^7
ρ_0	Contaminant density in the waste	g/g	[1] p64	1.5×10^{-3}	2.4×10^{-9}	1.5×10^{-3}	2.4×10^{-9}
H_f	Equivalent height of leachate	M	$d\rho_0/C_0$	3.14 (1-5)	1.2 (0.5-2)	3.14 (1-5)	1.2 (0.5-2)
t_{GM}	Geomembrane thickness	M		0.0015	0.0015	0.0015	0.0015
t_{PL}	Primary liner thickness	M		0.75 (0.25-1.5)	0.75 (0.25-1.5)	0.007 (0.007; 0.01)	0.007 (0.007; 0.01)
t_{AL}	Attenuation layer thickness	M		3	3	3.75	3.75
t_{AQ}	Aquifer thickness	M		1	1	1	1
n_{PL}	Primary liner porosity		[4]; [6]	0.4	0.4	0.7	0.7
n_{AL}	Attenuation layer porosity			0.35	0.35	0.35	0.35
n_{AQ}	Aquifer porosity			0.3	0.3	0.3	0.3
w	Width of defect	m		0.3 (0.1-0.5)	0.3 (0.1-0.5)	0.3 (0.1-0.5)	0.3 (0.1-0.5)
f	Frequency of defects	defect/ha	[1] p427	2.5 (1-5)	2.5 (1-5)	2.5 (1-5)	2.5 (1-5)
k_{PL}	Primary liner hydraulic conductivity	m/s		10^{-9} (10^{-10} - 10^{-8})	10^{-9} (10^{-10} - 10^{-8})	5×10^{-11} (5×10^{-12} - 5×10^{-9})	5×10^{-11} (5×10^{-12} - 5×10^{-9})
k_{AL}	Attenuation layer hydraulic conductivity	m/s		10^{-7} (10^{-8} - 10^{-6})			
θ_x	Transmissivity geomembrane-primary liner	m ² /s	[3]	1.6×10^{-8} (10^{-9} - 10^{-7})	1.6×10^{-8} (10^{-9} - 10^{-7})	10^{-10} (10^{-11} - 10^{-9})	10^{-10} (10^{-11} - 10^{-9})
D_{GM}	Diffusion coefficient in geomembrane	m ² /s	[1] p295	5×10^{-15}	5×10^{-16}	5×10^{-15}	5×10^{-16}
D_{PL}	Diffusion coefficient in primary liner	m ² /s	[1] p270,394	6×10^{-10} (6×10^{-11} - 3×10^{-9})	4×10^{-10} (6×10^{-11} - 3×10^{-9})	3×10^{-10} (6×10^{-11} - 3×10^{-9})	3×10^{-10} (6×10^{-11} - 3×10^{-9})
D_{AL}	Diffusion coefficient in attenuation layer	m ² /s	[1] p270	7.5×10^{-10} (4.2×10^{-11} - 7.5×10^{-9})	4.2×10^{-10} (4.2×10^{-11} - 7.5×10^{-9})	7.5×10^{-10} (4.2×10^{-11} - 7.5×10^{-9})	4.2×10^{-10} (4.2×10^{-11} - 7.5×10^{-9})
D_{AQ}	Mechanical dispersion in aquifer	m ² /s	[1] p270	100	100	100	100
ρ_{PL}	Primary liner dry density	kg/m ³		1240	1240	790	790
K_{dPL}	Primary liner sorption coefficient	m ³ /kg	[4]; [5]	0	0.00044	0	0.072
K_{dAL}	Attenuation layer sorption coefficient	m ³ /kg	[1] p270	0	0	0	0
v_{AQ}	Horizontal Darcy velocity in aquifer	m/y		1	1	1	1
h_{pt}	Leachate height in waste	m		0.3	0.3	0.3	0.3
h_{pb}	Hydraulic pressure in the aquifer*	m		3.75	3.75	3.75	3.75

[1] Rowe et al. (2004); [2] O. Reg 232/98; [3] Touze-Foltz and Barroso (2006) ($\log \theta = -2.2322 + 0.7155 \log K_{GCL}$); [4] Shackelford and Daniel (1991); [5] Lo et al. (2000); [6] Kim et al. (1997);

*In sensitivity analyses involving change of thickness of the primary liner, values of h_{pb} are modified so as to maintain hydraulic gradient at its base-case value of 0.08%.

2.3 LIMITATIONS OF ANALYSES

The interpretive scope of our analyses is clearly constrained by the assumptions underlying them. The mathematical equations presented earlier simulate single-species, single-phase transport. The wide range of possible combinations of species and phases, and associated uncertainties, does not allow our simulations to take them into account, unless a specific scenario is being studied. Our ultimate goal is to compare different design configurations and our analyses must therefore remain reasonably general in scope.

Partial saturation usually leads to lower hydraulic conductivity, provided the liner is not dehydrated and desiccated, say as a result of strong thermal gradients (Azad et al., 2012; Abuel-Naga et al., 2013; El-Zein et al., 2014). Any loss of functionality of the drainage system can lead to the build-up of higher pressure heads on top of the liner and therefore higher seepage velocities and advective flux. Non-linear sorption can lead to lower levels of sorption, relative to the linear case, and hence more contamination risk for groundwater. Non-equilibrium sorption can have a similar effect, though it is unlikely to be significant over the large time scales of concern. Acidity and redox potential are important factors, not considered here, in the mobility of heavy metals. As mentioned earlier, sorption has been conservatively assumed to be absent in the attenuation layer. Key boundary conditions in our analyses are clearly oversimplifications of likely site conditions. This is especially the case for the aquifer downstream boundary condition (and aquifer hydraulic regime) which assume that contaminants are discharged from the system at the advective rate, hence neglecting dispersive effects at the boundary. On the positive side, the condition is likely to be conservative, keeping more contaminants in the system than would otherwise be the case. The assumption of regular and parallel wrinkles is unlikely to be true; however, the wide range of possible scenarios is difficult to cover and would require much more elaborate 3D analyses.

Finally, we have made two assumptions that are likely to have the most significant impacts on our conclusions. First, the contaminants in the waste are taken to be fully available for migration into the underlying liner when in fact inorganic chemicals can become immobilised at the source. This is however a conservative assumption. Second, the parameters we have used in the analyses are taken to be time-independent, as though no deterioration of the system components take place over time. This is clearly not the case, especially since peak concentrations in the aquifer, according to our analyses, are reached sometimes hundreds of years after waste placement on landfill closure. There is no guarantee, for example, that geomembranes will remain chemically intact over timeframes of centuries. Therefore, it is important to interpret our results as guidance for comparative designs under idealised conditions, rather than predictions of actual behaviour for centuries to come.

3. RESULTS

3.1 GENERAL BEHAVIOUR OF BASE CASE

3.1.1 Introduction

In analysing results, the maximum value of $C(x,y,t)$ in the aquifer was identified (referred to henceforth as maximum concentration C_{max}). Given the aquifer's relatively large mechanical dispersivity and small thickness, the concentration was found to be constant along the y direction (perfect mixing) and all results shown are taken at midpoint across the depth of the aquifer. Maximum $C(x,t)$ (i.e., C_{max}) was determined by visually examining graphical plots of data.

The general hydraulic and chemical behaviours of each landfill liner for the base case are shown in Figures 3 and 4. Figure 3 displays the downward Darcy velocity for CCL and GCL, whilst Figure 4 shows the levels of contamination within the aquifer at three different times; $t=50, 200$ and 600 years. From Figure 3, it can be seen that leakage occurs over a wider area in the case of CCL relative to GCL. This is due to its high transmissivity at the interface with the geomembrane. It is also evident from Figure 4 that as time progresses the maximum peak concentrations that occur beneath the wrinkles in earlier years are smoothed out. This is indicative of the strong effect of mechanical dispersion in the aquifer. Note that the concentration levels are also affected by the magnitude of groundwater flow in the aquifer and the maximum contamination levels are reached at, or close to, the downstream end of the landfill. Similar effects were found by El-Zein and Rowe (2008) and El-Zein et al. (2012) for organic contaminants. Peaks of inorganic contamination in the groundwater are reached over 500 years after the operation of the landfill, well beyond the service life of the geomembrane. This is consistent with earlier findings by Rowe and Brachman (2004).

Next, the effects of changing a number of different parameters are considered. The chemical performance of the liner is expressed by the ratio of maximum concentration of contaminant (chloride or cadmium) encountered in the aquifer to its initial concentration in the waste. The patterns of variability for chloride and cadmium are very similar. Therefore, we will show graphs for the case of chloride only, unless notable differences are found for cadmium.

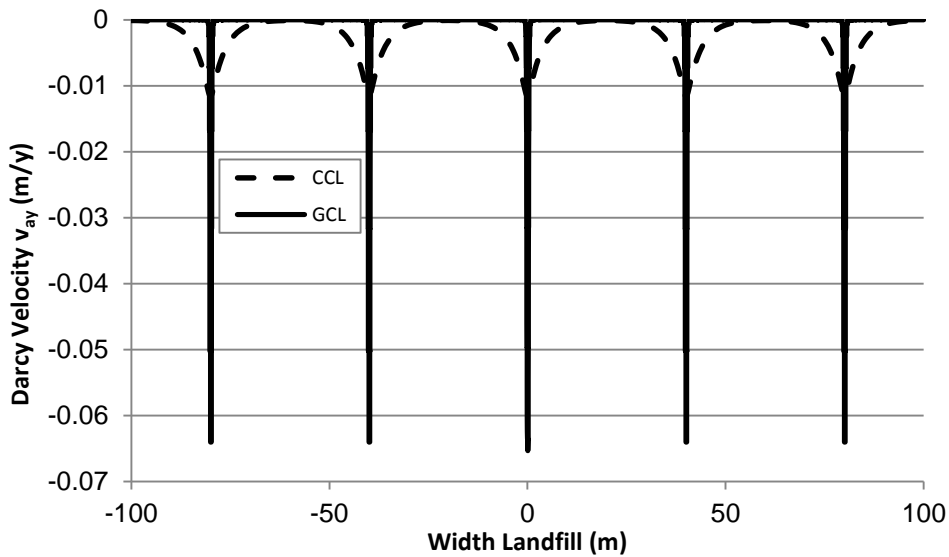


Figure 3. Horizontal profile of downward Darcy velocity at the lower surface of the primary liner for CCL, base case a, and GCL, base case c.

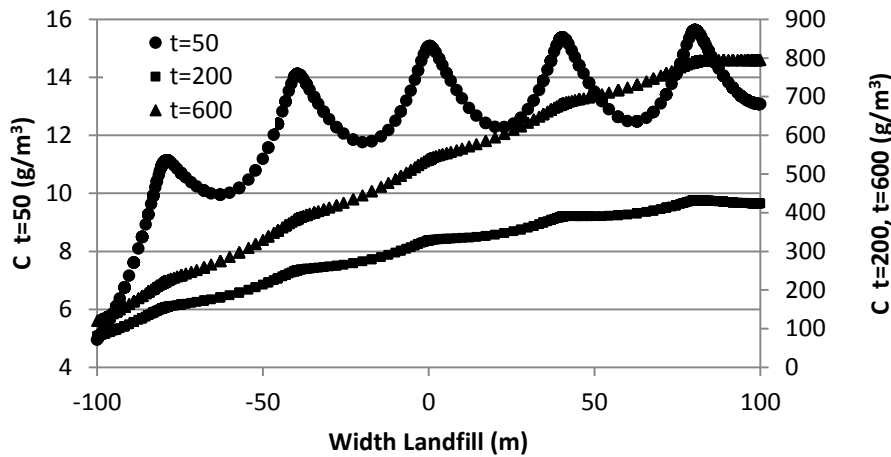


Figure 4. Horizontal profiles of concentration in the aquifer at $t=50$, 200 and 600 years for base case a. (the corresponding curves for base cases b, c and d are qualitatively similar to the one shown here)

3.1.2 Effects of Depth of Primary Liner

The effects of changing PL depths, while maintaining the same hydraulic gradient as the base case, are shown in Figure 5 for chloride transport through a CCL system. Both leakage and chemical concentrations decline in a non-linear fashion as thickness increases, with smaller effects observed at larger thicknesses. The drop in maximum concentration is more dramatic than that of leakage rates. This is because concentration in the groundwater under a thicker PL is affected by both smaller leakage rates (therefore less advective transport) and a thicker barrier against molecular diffusion.

In the case of the GCL system, only two different depths are usually of relevance and have been considered here: 7 mm and 10 mm. The effect of switching to a larger thickness can be glimpsed from Table 4 and, as expected, both leakage and maximum concentration decline with increasing depth for both chloride and cadmium.

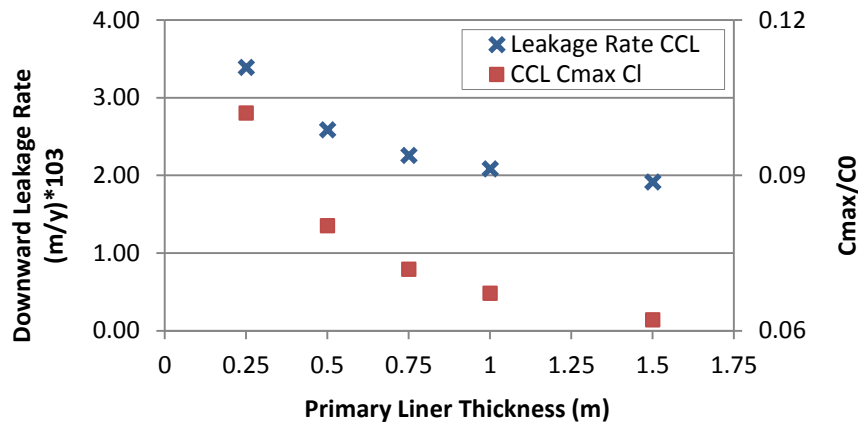


Figure 5. Change in leakage rates and maximum contaminant concentrations with the depth of the primary liner, CCL Chloride (under constant hydraulic gradient of 8%)

3.1.3 Effects of Hydraulic Conductivities and Transmissivity

The effects of varying the hydraulic conductivities of the PL and AL are shown in Figures 6 and 7, respectively. In Figures 6a and 6b, both leakage rates and contamination levels increase exponentially with the PL's hydraulic conductivity, highlighting the importance of this design parameter. Figure 7, on the other hand, shows that leakage rates and maximum concentrations grow rapidly with the hydraulic conductivity of the AL, with significant gains predicted if the hydraulic conductivity drops from 10^{-7} m/s to 10^{-8} m/s.

Figures 8a and 8b show the effects of changing the transmissivity for the interface between the geomembrane, on the one hand, and the CCL or GCL, on the other hand. Both figures show, as expected, an increase in leakage rates and maximum concentrations with transmissivity. However, in the case of the CCL where the transmissivity is generally higher, an inflection in the curve occurs between the transmissivity values of 10^{-8} and 10^{-6} m²/s with both leakage and maximum concentration stabilising for values greater than 10^{-6} m²/s. This is possibly due to the fact that, as transmissivity increases, interaction between consecutive defects counteracts the increase in leakage. This is likely the case beyond a certain value of transmissivity which, in the case of the GCL, is not reached here, interaction doesn't occur and no inflection is observed in the curves.

3.1.4 Effects of Width and Frequency of Defects

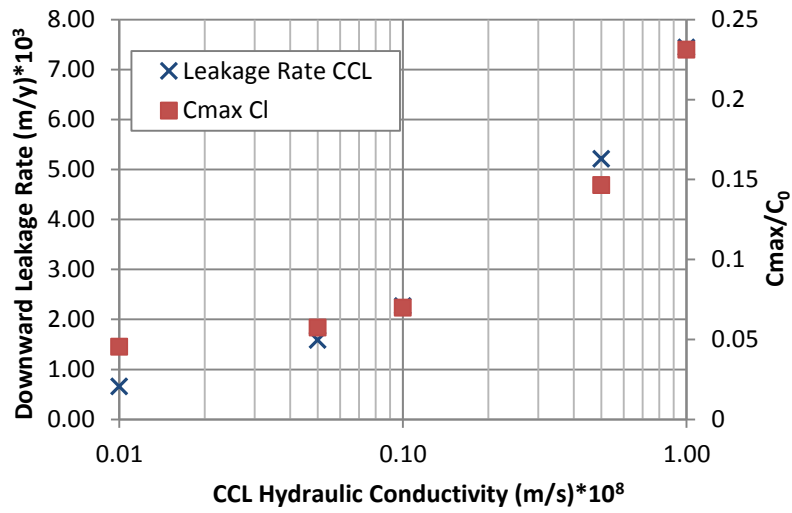
Figures 9a and 9b depict the change in leakage rates and maximum concentrations with width and frequency of defects, respectively, for the case of chloride transport through the CCL system. The figures clearly reveal a linear relationship with leakage and contamination, as expected, increasing at a constant rate with defects width and frequency. This is an agreement with findings by El-Zein et al. (2012) for organic contaminants.

3.1.5 Effects of Equivalent Height of Leachate

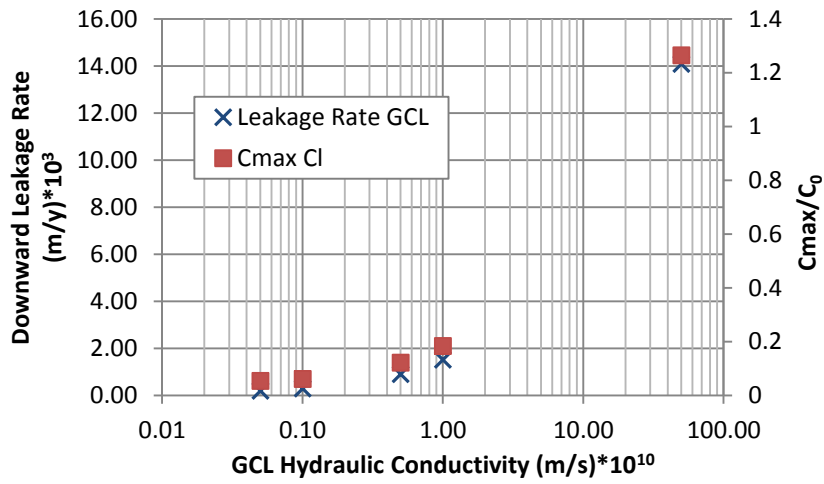
The equivalent height of leachate H_f reflects the total amount of contaminant accepted into the landfill and depends on, in addition to the total amount of waste, its content in contaminants (see equation 16). The effects of changing H_f are shown in Figure 10. Since H_f is a variable affecting chemical transport but not hydraulic flow, the leakage rates are not influenced by it. The maximum concentration of contaminant in the aquifer, as expected, increases with increasing H_f , although the rate of increase declines with higher H_f . At very high H_f , the system becomes dominated by a boundary condition akin to a constant concentration on top of the liner, and the maximum concentration in the aquifer is partly determined by the rate at which the contaminants are flushed out of the system, i.e. the aquifer's downstream boundary condition which, in this simulation, is an advective discharge boundary condition.

3.1.6 Effects of Molecular Diffusion

Figures 11a, 11b, 12a and 12b, depict the effects of changing the molecular diffusion coefficient of the primary liner and the attenuation layer, for the CCL and GCL systems. Once again, as diffusion coefficients are chemical and not hydraulic parameters, leakage rates remain constant in these figures. As expected, higher diffusion coefficients yield higher concentrations of contaminant in the aquifer. The curve, in the case of CCL, appears to be exponential with the rate of change increasing as the diffusion coefficients increase.



a. Case a: CCL



b. Case c: GCL

Figure 6. Leakage rates and maximum contaminant concentrations versus hydraulic conductivity of liner

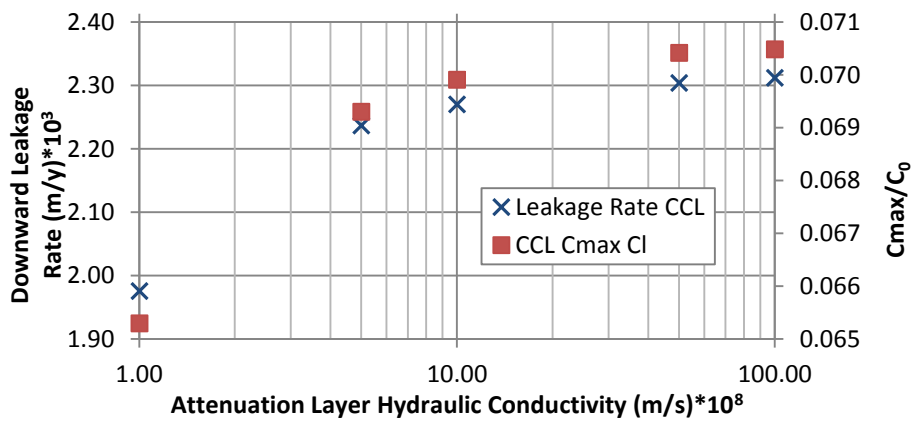
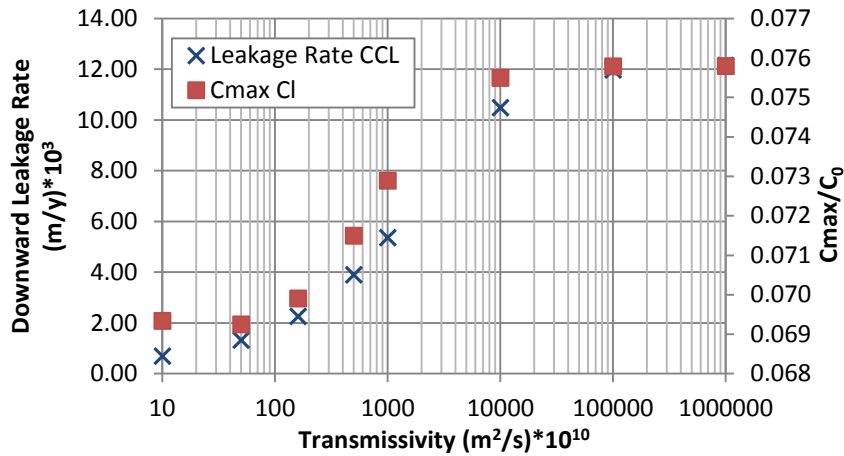
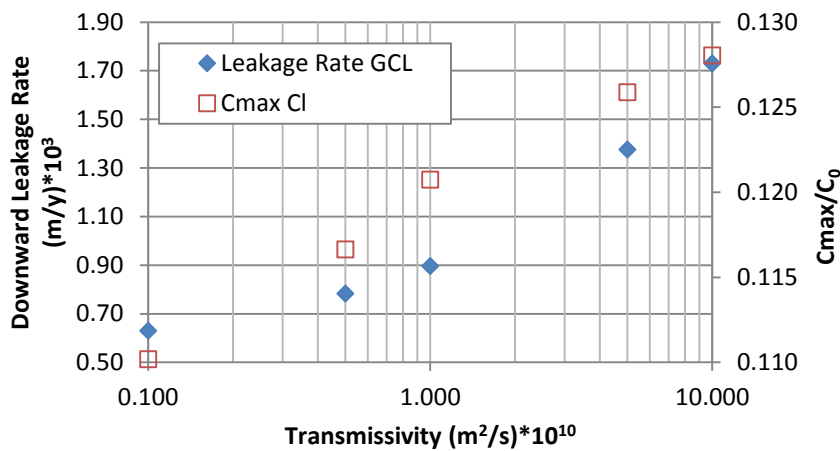


Figure 7. Change in leakage rates and maximum contaminant concentrations with the hydraulic conductivity of the attenuation layer, CCL case a.



a. Case a: CCL



b. Case c: GCL

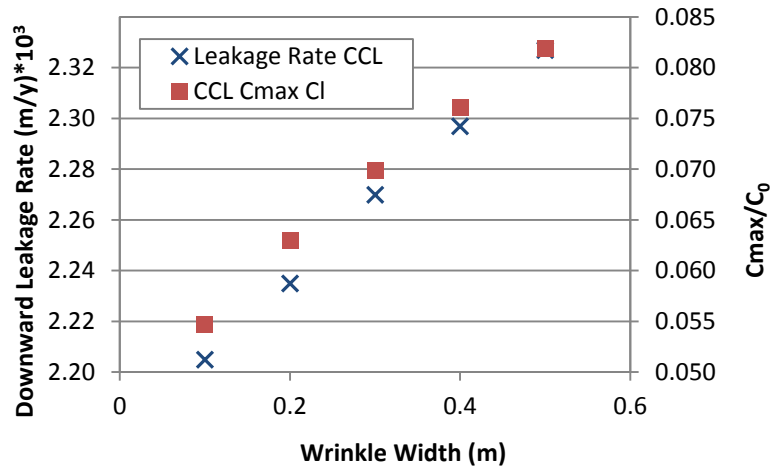
Figure 8. Leakage rates and maximum contaminant concentration versus geomembrane-liner transmissivity

3.1.7 Comparison of the Effects of Different Design Parameters

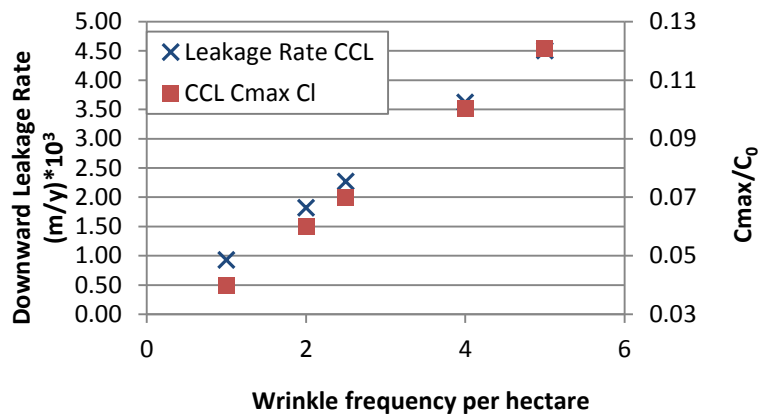
So far, we have examined changes to leakage rates and C_{max} as various design or field parameters change. This allows us to make a *qualitative* judgement about the relationship between each parameter and these performance indicators. However, we have not been able to compare the *magnitude* of change for two or more parameters. In order to do so, we calculate variability ratios R_{vL} and R_{vC} , defined in Table 2, which provide an estimate of the average percentage change in leakage rates and C_{max} , respectively, per percentage change in a given parameter. The larger R_{vL} and R_{vC} , the more impact the parameter has on the indicators. Tables 3 and 4 show R_{vL} and R_{vC} for 9 parameters. These ratios must be interpreted cautiously as they are averaged over a given range and depend on the range chosen.

For the CCL, the width of the defect has only a small impact on leakage rates; however, it has a sizeable influence on chemical concentrations in the aquifer because it determines the extent of direct contact between leachate in the waste and the primary liner. Changes to the hydraulic conductivity of the AL, within the specified range, have a relatively small impact on both leakage and concentration, for CCL and GCL liners. In CCL liners, deviations from the base-case diffusion coefficient of the contaminant in the PL appear to have a more pronounced effects on C_{max} than those derived from the diffusion coefficient of the AL. This conclusion is reversed in the case of GCL because the bentonite clay buffer in the GCL is thin (7 or 10 mm) and the AL plays a more prominent role as a shield against diffusion.

All in all, changes to the frequency of defects in the geomembranes and the hydraulic conductivity of the primary liner (in both CCLs and GCLs) have the strongest effects on leakage and/or concentrations. In addition, the effects of increasing the thickness of the CCL are quite important. Combining variability ratios with cost per unit change in a given design parameter would allow landfill designers to optimise designs in order to achieve desired environmental outcomes at the lowest possible cost.



a. Effect of width



b. Effect of frequency

Figure 9. Leakage rates and maximum contaminant concentrations versus wrinkle width and frequency for case a CCL

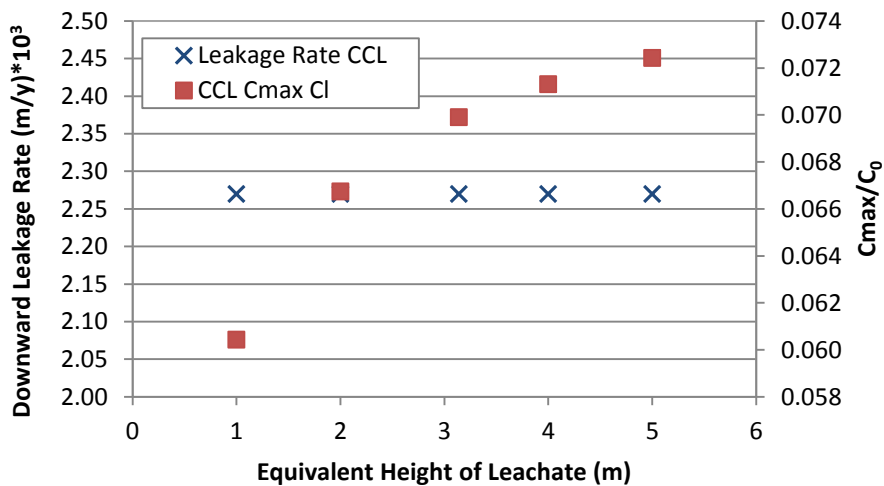
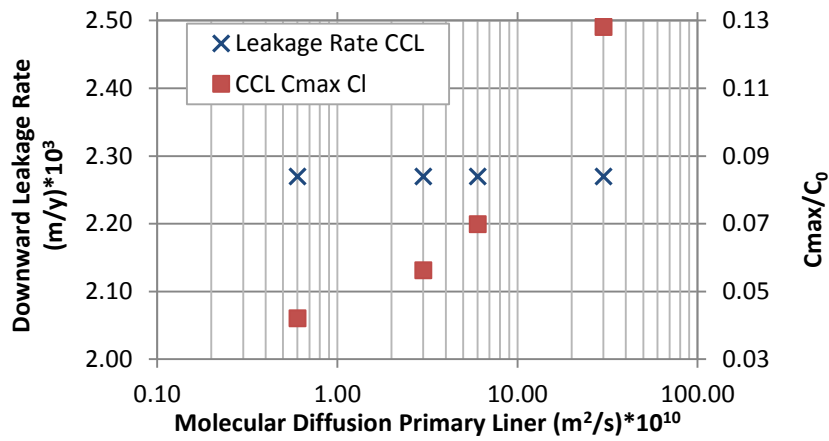
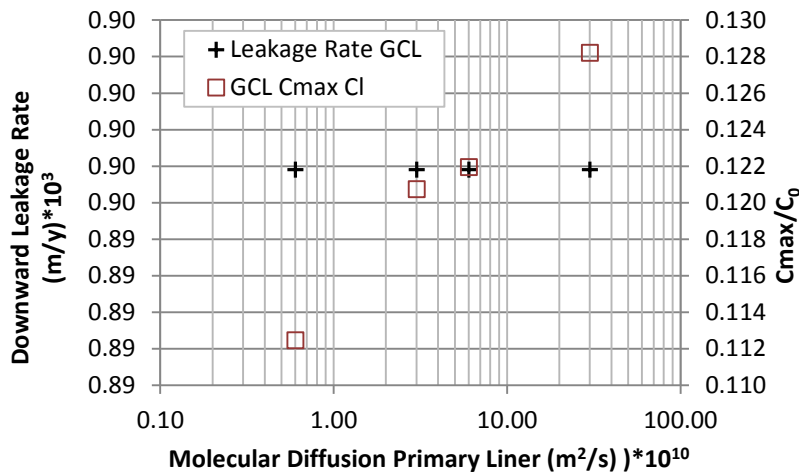


Figure 10. Change in leakage rates and maximum contaminant concentration with the density of chloride in the waste p_0 , CCL case a.



a. Case a: CCL



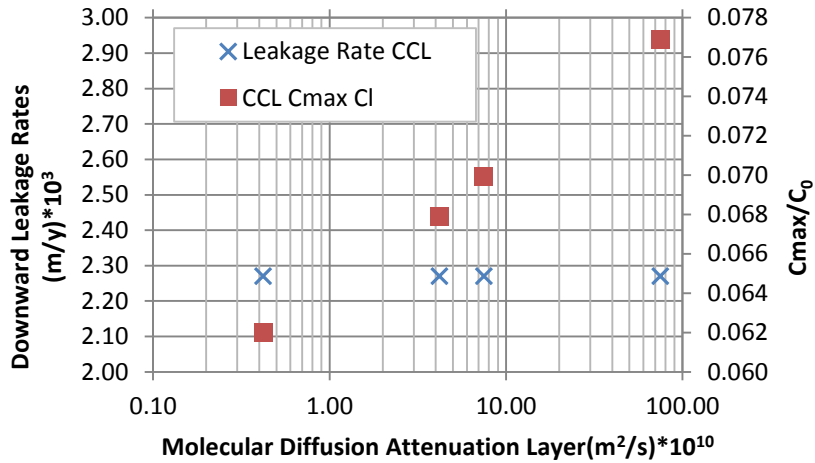
b. Case c: GCL

Figure 11. Leakage rates and maximum concentrations versus molecular diffusion coefficient in primary liner

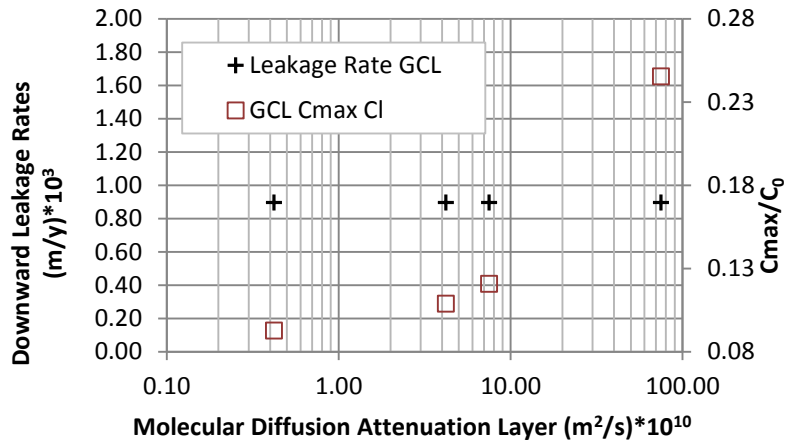
3.1.8 Leakage Rate as Predictor of Maximum Chemical Concentration in the Aquifer

Tables 3 and 4 show the ratio $R_{LC}=R_{vL}/R_{vC}$ which reflects the extent to which changes in leakage rates are proportional to changes in chemical concentrations. Predictably, H_f and diffusion coefficients have no impact on leakage rates, therefore yielding $R_{LC}=0$. Changes in leakage rates as a result of changes in the frequency of defects and hydraulic conductivity of the primary liner correlate well with corresponding changes in maximum chemical concentrations in the aquifer. This is also the case for the width of defects in GCL but not in CCL.

On the other hand, changes in transmissivities have a smaller effect on concentrations in the aquifer than may be implied by their strong effects on leakage rates. This is surprising since no such effect is observed when varying k_{PL} . In order to explore this behaviour further, we show in Figure 13, horizontal profiles of downward Darcy velocity at the interface between the CCL liner and the attenuation layer, for two cases of chloride transport having similar leakage rates but very different maximum chemical concentrations in the aquifer. The only differences in input data to the two cases are the respective values of k_{PL} and θ_x . It is clear from the figure that, although leakage rates in the two cases are very close, Darcy velocity profiles are very different. It is worthwhile remembering here that the leakage rate is a measure of Darcy velocity, *averaged* over the surface area below the liner (equation 17). It is obvious from the figure that another key parameter here is $V_{ay,max}$, the maximum Darcy velocity under each defect which has a strong effect on the downward flux of contaminants and, at least partly, explain the observed differences in maximum concentrations. Unfortunately, $V_{ay,max}$ is not usually taken into account in landfill analysis and design; nor is it easily measurable in situ especially since it is likely to be variable in space and time. Clearly, therefore, leakage rates only show part of the picture and chemical concentrations need to be considered in critical cases.



a. Case a: CCL



b. Case c: GCL

Figure 12. Leakage rates and maximum concentrations versus molecular diffusion of attenuation layer

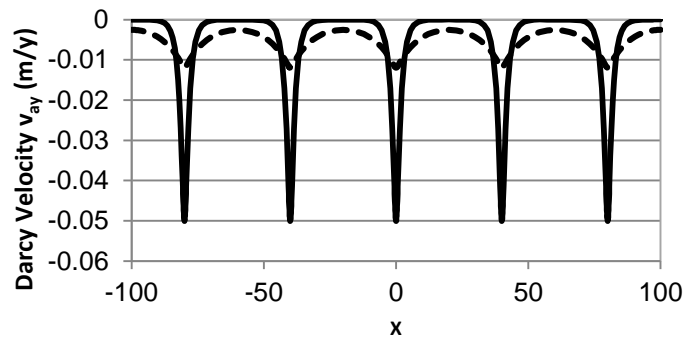


Figure 13. Horizontal profile of downward Darcy velocity at the lower surface of the primary liner for two variants of CCL case a (chloride): i. $k_{PL}=10^{-9}$ m/s; $\theta_x=10^{-7}$ m²/s; leakage rate= 5.37×10^{-3} m/y; $v_{aymax}=1.5 \times 10^{-2}$ m/y; $C_{max}=871$ g/m³ (dashed line) and ii. $k_{PL}=5 \times 10^{-9}$ m/s; $\theta_x=1.6 \times 10^{-8}$ m²/s; leakage rate= 5.22×10^{-3} m/y; $v_{aymax}=5 \times 10^{-2}$ m/y; $C_{max}=1753$ g/m³ (solid line)

Table 2. Definitions of Variability Ratios R_v

Variable	Description			Definition	Significance
p^*	Design parameter range	p_{min}	p_{max}		
L	Leakage rate calculated at the 2 ends of the parameter range	L_1	L_2		
C_{max}	Maximum concentration in aquifer calculated at the 2 ends of the parameter range	C_{max1}	C_{max2}		
Δp	Percent change in p			$\frac{p_{max} - p_{min}}{p_{max}}$	
ΔL	Percent change in L			$\frac{L_2 - L_1}{L_2}$	
ΔC	Percent change in C			$\frac{C_{max2} - C_{max1}}{C_{max2}}$	
$R_{vLeakage}$	Variability ratio for leakage rate	Average % change in leakage rate per 1% change in design parameter		$\frac{\Delta L}{\Delta p}$	<ol style="list-style-type: none"> +ve R_{vL}: leakage increases with increasing p -ve R_{vL}: leakage declines with increasing p The greater R_{vL}, the stronger the effect of p on L
R_{vCmax}	Variability ratio for maximum concentration in aquifer	Average % change in aquifer maximum concentration per 1% change in design parameter		$\frac{\Delta C}{\Delta p}$	<ol style="list-style-type: none"> +ve R_{vC}: C_{max} increases with increasing p -ve R_{vC}: C_{max} declines with increasing p The greater R_{vC}, the stronger the effect of p on C_{max}
R_{LC}	Ratio of variability ratios	Average % change in leakage rate per 1% change in aquifer maximum concentration		$\frac{R_{vLeakage}}{R_{vCmax}}$	The closer R_{LC} is to 1, the better leakage as a qualitative predictor of maximum chemical concentrations in the aquifer.

* p can be any one of the following design parameters: H_f , t_{PL} , w, f, k_{PL} , KAL , θ , D_{PL} , D_{AL} .

4. CONCLUSIONS

We have simulated the transport of chloride and cadmium through composite liners with multiple defects in the geomembrane. Levels of inorganic contamination in the aquifer are found to be most sensitive to the hydraulic conductivities of the primary liners, the frequency of defects and, in the case of the CCL, the depth of the primary liner. It is also clear from these results that the use of the hydraulic regime to estimate the levels of contamination in the aquifer can, in some instances, be insufficient. This is most pronounced in the effects of change in transmissivity: reductions in leakage rates as a result of a decrease in the value of transmissivity (i.e., improvement in the quality of contact between geomembrane and primary liner) do not translate into a proportionate decline in maximum inorganic contamination levels in the aquifer.

Overall, the time it takes concentrations in the aquifer to reach their maxima, under the idealised conditions of this study, is measured in centuries rather than decades. Hence, the long-term performance and durability of the liner will have a stronger impact in the case of inorganic contaminants, relative to organic ones. Equally, the design time horizon, usually set by regulatory agencies, is an important consideration and different time horizons can lead to different conclusions as to whether the liner is achieving its objectives or not. Inorganic contaminants, unlike organic ones, tend to remain for a long time in the waste-landfill system in which they have been deposited. Hence, regulatory periods of compliance (e.g., 35 or 50 years) can miss an important part of the picture and, in effect, transmit the problem to future generations.

Table 3. Variability Ratios R_v for the CCL

		H_f	t_{PL}	w	f	k_{PL}	k_{AL}	θ	D_{PL}	D_{AL}
Parameter Range	Minimum	1 m (Cl)	0.25 m	0.1 m	1 wr/ha	10^{-10} m/s	10^{-8} m/s	10^{-9} m/s	6×10^{-11} m/s	4.2×10^{-11} m/s
		0.5 m (Cd)								
Parameter Range	Maximum	5 m (Cl)	1.5 m	0.5 m	5 wr/ha	10^{-8} m/s	10^{-6} m/s	10^{-7} m/s	3×10^{-9} m/s	7.5×10^{-9} m/s
		2 m (Cd)								
Output for CCL-Cl	$L_1 (10^{-3}$ m/year)	2.27	3.39	2.21	0.93	0.667	1.98	0.698	2.27	2.27
	$L_2 (10^{-3}$ m/year)	2.27	1.92	2.33	4.51	7.45	2.31	12.20	2.27	2.27
	$C_1 (g/m^3)$	722.20	1219.50	654.10	476.10	544.90	780.30	828.60	503.30	740.80
	$C_2 (g/m^3)$	865.60	742.45	978.30	1443.20	2765	842.30	905.80	1531.00	918.80
	$R_{yLeakage}$	0.00	-0.92	0.06	0.99	0.92	0.15	0.88	0.00	0.00
	R_{yCmax}	0.21	-0.77	0.41	0.84	0.81	0.07	0.05	0.68	0.19
	$R_{LC} = R_{yLeakage} / R_{yCmax}$	0.00	1.20	0.15	1.18	1.14	2.14	17.60	0.00	0.00
Output for CCL-Cd	$L_1 (10^{-3}$ m/year)	2.27	3.42	2.21	0.93	0.667	1.98	0.698	2.27	2.27
	$L_2 (10^{-3}$ m/year)	2.27	1.915	2.33	4.51	7.45	2.31	12.20	2.27	2.27
	$C_1 (g/m^3)$	1.85	0.004	1.44	0.925	0.994	1.87	1.98	1.23	2.24
	$C_2 (g/m^3)$	2.18	0.002	2.59	4.03	9.80	2.10	2.32	4.69	2.26
	$R_{yLeakage}$	0.00	-0.95	0.06	0.99	0.92	0.15	0.88	0.00	0.00
	R_{yCmax}	0.20	-1.46	0.55	0.96	0.91	0.11	0.12	0.76	0.01
	$R_{LC} = R_{yLeakage} / R_{yCmax}$	0.00	0.65	0.11	1.03	1.01	1.36	7.33	0.00	0.00

Table 4. Variability Ratios R_v for the GCL

		H_f	t_{PL}	w	f	k_{PL}	k_{AL}	θ	D_{PL}	D_{AL}
Parameter Range	Minimum	1 m (Cl)	0.007 m	0.1 m	1 wr/ha	10^{-12} m/s	10^{-8} m/s	10^{-11} m/s	6×10^{-11} m/s	4.2×10^{-11} m/s
		0.5 m (Cd)								
Parameter Range	Maximum	5 m (Cl)	0.01 m	0.5 m	5 wr/ha	10^{-9} m/s	10^{-6} m/s	10^{-9} m/s	3×10^{-9} m/s	7.5×10^{-9} m/s
		2 m (Cd)								
Output for GCL-Cl	$L_1 (10^{-3}$ m/year)	0.90	0.91	5.72	3.60	1.83	6.59	6.30	8.96	8.96
	$L_2 (10^{-3}$ m/year)	8.96	0.69	12.10	17.90	141.00	9.30	17.30	8.96	8.96
	$C_1 (g/m^3)$	1132.60	1439.38	886.30	743.50	627.90	1169.10	1316.60	13.44	1108.30
	$C_2 (g/m^3)$	1326.00	1178.80	1928.50	2448.60	15104.40	1466.20	1530.00	1531.90	2931.80
	$R_{yLeakage}$	0.00	-0.39	0.66	1.00	0.99	0.29	0.64	0.00	0.00
	R_{yCmax}	0.18	-0.27	0.68	0.87	0.96	0.20	0.14	0.13	0.63
	$R_{LC} = R_{yLeakage} / R_{yCmax}$	0.00	1.46	0.97	1.15	1.03	1.45	4.57	0.00	0.00
Output for GCL-Cd	$L_1 (10^{-3}$ m/year)	8.96	0.90	5.72	3.60	1.83	6.59	6.30	8.96	8.96
	$L_2 (10^{-3}$ m/year)	8.96	0.6892	12.10	17.90	141.00	9.30	17.30	8.96	8.96
	$C_1 (g/m^3)$	2.96	0.004	2.22	1.88	1.21	3.05	3.49	3.61	4.11
	$C_2 (g/m^3)$	4.29	0.003	5.36	6.41	45.40	3.97	4.24	4.15	8.77
	$R_{yLeakage}$	0.00	-0.32	0.66	1.00	0.99	0.29	0.64	0.00	0.00
	R_{yCmax}	0.41	-0.32	0.73	0.88	0.97	0.23	0.18	0.13	0.54
	$R_{LC} = R_{yLeakage} / R_{yCmax}$	0.00	1.00	0.90	1.14	1.02	1.26	3.56	0.00	0.00

REFERENCES

1. Abuel-Naga, H.M., Bouazza, A., 2009. Numerical characterization of advective gas flow through GM/GCL composite liners having a circular defect in the geomembrane. *Journal of Geotechnical and Geoenvironmental Engineering* **135**:1661-1671.
2. Abuel-Naga, H.M., Bouazza, A., Gates, W.P., 2013. Impact of bentonite form on the thermal evolution of the hydraulic conductivity of geosynthetic clay liners, *Geotechnique Letters* **3**, ICE Publishing, London UK, pp. 26-30.
3. Azad F.M., El-Zein A., Rowe R.K., Airey D.W. 2012. Modelling of thermally induced desiccation of geosynthetic clay liners in double composite liner systems. *Geotextiles and Geomembranes* **34**:28-38.
4. Booker JR, Rowe RK., 1987. One dimensional advective-dispersive transport into a deep layer having a variable surface concentration. *International Journal of Numerical and Analytical Methods in Geomechanics*, **11**(2), 131-142.
5. Chappel, M.J., W.A. Take, W.A., Brachman, R.W.I., Rowe, R.K., 2008. A Case Study of Wrinkles in a Textured HDPE Geomembrane on a Slope. *GEOAMERICAS 2008*, Cancun, Mexico, March, 452-458.
6. El-Zein, A. 2005. Exponential finite elements for diffusion-advection problems. *International Journal for Numerical Methods in Engineering* **62**(15):2086-2103.
7. Elzein AH, Booker JR. 1999. Groundwater pollution by organic compounds: a two-dimensional analysis of contaminant transport in stratified porous media with multiple sources of non-equilibrium partitioning. *International Journal for Numerical and Analytical Methods in Geomechanics* **23**(14):1717-1732.
8. El-Zein AH, Carter JP, Airey DW. 2005. Multiple-porosity contaminant transport by finite-element method. *International Journal of Geomechanics* **5**(1):24-36.
9. El-Zein, A. 2008. A general approach to the modelling of contaminant transport through composite landfill liners with intact or leaking geomembranes. *International Journal for Numerical and Analytical Methods in Geomechanics*, **32**(3):265-287.
10. El-Zein, A., Rowe, R.K., 2008. Impact on groundwater of concurrent leakage and diffusion of dichloromethane through geomembranes in landfill liners. *Geosynthetics International* **15**(1):55-71.
11. El-Zein, A. and Touze-Foltz N. 2010. Equivalency of Landfill Liner Designs, including Clay Liners, Geosynthetics Liners and Polymer-Enhanced Mineral Barriers, under French Legislation. *International Conference on Geosynthetics*, Guarujá, Brazil, 2010.
12. El-Zein A and Balaam N. 2012. Saturated-unsaturated flow and solute transport in engineered liner systems: a new special-purpose finite-element analysis software. *Australian Geomechanics Journal*, **47**(3):11-126.
13. El-Zein, A., McCarroll, I., Touze-Foltz, N., 2012. Three-dimensional finite-element analyses of seepage and contaminant transport through composite geosynthetics clay liners with multiple defects. *Geotextiles and Geomembranes* **33**:34-42.
14. Foote JG, Benson CH, Tunser BE. 2002. Comparison of solute transport in 3 composite liners. *Journal of Geotechnical and Geoenvironmental Engineering* **128**(5):391-403.
15. Giroud, J.P., Touze-Foltz, N., 2005. Equations for calculating the rate of liquid flow through geomembrane defects of uniform width and finite or infinite length. *Geosynthetics International* **12**:191-204.
16. Nosko, V., Touze-Foltz, N., 2000. Geomembrane liner failure: modelling of its influence on contaminant transfer. *Proceedings Eurogeo 2, Second European Conference on Geosynthetics*, Bologna, Italia, 15-18 October 2000, 557-560.
17. Ogata A., Banks R.B., 1961. A solution of the differential equation of longitudinal dispersion in porous media. *US Geological Survey, Professions Paper 411-A*.
18. Pelte, T., Pierson, P., Gourc, J.P., 1994. Thermal analysis of geomembrane exposed to solar radiation. *Geosynthetics International* **1**:21-44.
19. Rowe, R.K., Quigley, R.M., Brachman, R.W.I., Booker, J.R., 2004. *Barrier Systems for Waste Disposal Facilities*. Spon Press, London and New York, 587 pages.
20. Rowe, R.K. and Brachman, R.W.I., 2004. Assessment of equivalence of composite liners. *Geosynthetics International* **11**(4):273-286.
21. Rowe, R.K., 2005. Long term performance of contaminant barrier systems. *Géotechnique* **9**:631-678.
22. Touze-Foltz, N., Schmittbuhl, J., Memier, M., 2001. Geometric and spatial parameters of geomembrane wrinkles on large scale model tests. *Geosynthetics Conference 2001*, Portland, USA, 715-728.
23. Wilson-Fahmy, R.F., Koerner, R.M., 1995. Leakage rates through holes in geomembranes overlying geosynthetic clay liners. *Proceedings Geosynthetics '95, Industrial Fabrics Association International*, 655-668.